Calhoun: The NPS Institutional Archive

DSpace Repository

Theses and Dissertations | 1. Thesis and Dissertation Collection, all items

1949

Wideband phase shift networks for single sideband transmitters

Laden, Hyman Nathaniel

Annapolis, Maryland. Naval Postgraduate School

http://hdl.handle.net/10945/30444

This publication is a work of the U.S. Government as defined in Title 17, United States Code, Section 101. Copyright protection is not available for this work in the United States.

Downloaded from NPS Archive: Calhoun

http://www.nps.edu/library

Calhoun is the Naval Postgraduate School's public access digital repository for research materials and institutional publications created by the NPS community. Calhoun is named for Professor of Mathematics Guy K. Calhoun, NPS's first appointed -- and published -- scholarly author.

Dudley Knox Library / Naval Postgraduate School
411 Dyer Road / 1 University Circle
Monterey, California USA 93943

WIDEBAND PHASE SHIFT NETWORKS FOR SINGLE SIDEBAND TRANSMITTERS

H. N. LADEN

Library
U. S. Naval Postgraduate School
Annapolis, Md.

WIDEBAND PHASE SHIFT NETWORKS FOR SINGLE SIDEBAND TRANSMITTERS

By

Hyman Nathaniel Laden,
Lieutenant, United States Navy

Submitted in partial fulfillment
of the requirements
for the degree of
MASTER OF SCIENCE
in
Engineering Electronics

United States Naval Postgraduate School
Annapolis, Maryland
1949

This work is accepted as fulfilling

the thesis requirements for the degree of

MASTER OF SCIENCE

in

ENGINEERING ELECTRONICS

from the

United States Naval Postgraduate School

[redacted]

Austin R. Frey
Chairman

Department of Electronics and Physics

Approved:

[redacted]

Academic Dean

1133a

PREFACE

During the Spring of 1948, single sideband communication procedures began to be widely discussed in amateur radio circles. This was due to a radical simplification of existing single sideband techniques by a group of General Electric Company engineers, which work was extensively publicized. The foundation of these techniques was the application of cascades of the well known, Müller R-C phase shift networks and other more complex lattices derived from this prototype. The theoretical discussion of these networks appeared in December 1946 as the work of R. Dome of General Electric Company.

In the Spring of 1948, this work was first brought to the attention of the author, then a student at the United States Naval Postgraduate School, Annapolis, Maryland. It was immediately obvious that existing design procedures did not result in optimum performance.

The design procedure discussed here was first derived by the author in July of 1948 as a result of independent research stimulated by Dome's work, discussed in some detail below. In February 1949, he became aware for the first time of the work of D. G. C. Luck: "Properties of Some Wide-Band Phase-Splitting Networks", Proceedings of the Institute of Radio Engineers, volume 37, number 2, February 1949, pages 147-151. In this latter work is derived the results embodied in Figure 21 of the following paper. The method of derivation here differs

considerably from that of Luck and, because of the more detailed attention to underlying hypotheses, seems somewhat more general. Also, the method used here permits direct extension to multiple cascades of phase shift networks.

The work included here was done under the supervision of Professor J. Chaney, whose criticism and editorial comment is gratefully acknowledged.

TABLE OF CONTENTS

		Page
I.	General Theory and Requirements of Single Sideband Transmitters	1
	1. Introduction	1
	2. General Methods of Achieving SS in Transmission	3
II.	The Dome Wideband Phase Shift Networks	10
	1. Basic R-C Lattice	10
	2. The L-C Lattice	12
	3. The R-C Lattice	13
	4. The Dome Design Procedure	14
III.	First Refinement of Dome Design	17
IV.	Second Refinement of Dome Design	21

LIST OF ILLUSTRATIONS

		Page
Figure 1.	Output Level Versus Frequency of Sideband and Carrier for Uniform Modulation Level in Vestigial Sideband Operation.	27
Figure 2.	Filter Type Single Sideband Transmitter	27
Figure 3.	Simple Single Sideband Receiver	28
Figure 4.	Western Electric Single Sideband Transmitter	29
Figure 5.	Western Electric Single Sideband Receiver	30
Figure 6.	Phase Shift Single Sideband Suppressed Carrier Transmitter	31
Figure 7.	Balanced Phase Shift Single Sideband Suppressed Carrier Transmitter	31
Figure 8.	Vestigial Sideband Effects in Phase Shift Single Sideband Suppressed Carrier System	32
Figure 9.	Basic R-C Lattice	33
Figure 10.	Equivalent Circuit of Basic R-C Lattice, Single Stage	33
Figure 11.	L-C Lattice	34
Figure 12.	Equivalent Circuit for L-C Lattice	34
Figure 13.	Further Equivalent Circuit for L-C Lattice	34
Figure 14.	R-C Lattice	35
Figure 15.	Equivalent Circuit for R-C Lattice	35
Figure 16.	Further Equivalent Circuit for R-C Lattice	36
Figure 17.	Typical B Curves for Dome Designs	36
Figure 18.	Extension of Dome Design Procedure	37
Figure 19.	Archetypical B Curve for Optimum Performance	38
Figure 20.	Defective B Curve	38
Figure 21.	Further Extension of Dome Design	39
Figure 22.	Comparison of Identical Phase Shift Networks with Different Design Procedures	40

WIDEBAND PHASE SHIFT NETWORKS FOR SINGLE SIDEBAND TRANSMITTERS

Summary: There is an inherent simplicity and flexibility in single sideband systems employing phase shift not present in systems employing selective filters. Earlier designs of wideband phase shift networks for single sideband application were based on premises which inevitably led to less than optimum performance. Herein, a design procedure is evolved which, without additional complexity of circuit, yields optimum performance in the sense of maximum bandwidth factor for a given tolerable phase shift error or minimum phase shift error for a given bandwidth factor.

I. GENERAL THEORY AND REQUIREMENTS OF SINGLE SIDEBAND TRANSMITTERS

1. Introduction

The usual amplitude modulation (AM) transmitter output consists of power distributed in a carrier frequency and upper and lower sideband frequencies. At least one half the total power output is in the carrier. The intelligence is contained in the sidebands and there is complete duplication in the upper sidebands of the information contained in the lower sidebands. Hence, it seems feasible to save energy by suppressing both the carrier and one set of sidebands at the source.

At the same time, this single sideband suppressed carrier (SSSC) transmission results in doubling the available operational channels in the frequency spectrum. It is also found that SSSC operation results in remarkably good communicability where, under usual operation, there would be annoying cross-carrier heterodyning (Dawley 9, Cheek 8). Further, there is a potential 3 db gain in signal to noise ratio possible at the receiver for a single sideband system over an ordinary AM system (Cheek 6). There are still other advantages of SSSC peculiar to power line carrier transmission (Cheek 5), which will not be mentioned here.

There are several types of single sideband (SS) operation. First, SS may be considered from the standpoint of the spectrum characteristics of the output. In one type of SS transmission, one set of sidebands is suppressed; the carrier and the other set of sidebands is transmitted. In contrast with the usual AM transmitter, the carrier power level is usually much lower than that of the sideband power. That is, usually there is partial carrier suppression.

A second type of SS operation is referred to as vestigial sideband. That is, the output is almost entirely in the upper sidebands; however, the lowest of the upper sidebands are slightly attenuated and some of the lower sidebands appear in the output at an even more attenuated level (Figure 1)*. Of course, this whole curve could be reflected about the carrier frequency, with the role of upper and lower sidebands interchanged.

*All illustrations appear in a section following the text.

Still another type of SS operation is referred to as suppressed carrier (SSSC). Both the carrier and one set of sidebands are suppressed and only the other set of sidebands is transmitted.

2. General Methods of Achieving Single Sideband in Transmission

One obvious way of suppressing one set of sidebands (and carrier) is the "brute force" technique, i.e. the employment of filters or other highly selective networks. This method was, in fact, used in the earliest SB transmitters described by J. R. Carson in 1915 (Carson 4) and still in essence used in existing Western Electric Company systems (Blackwell 2, Almquist 1). The chief difficulty is in the design of filters with the sharp cut-off characteristics required. Two such systems are sketched in Figures 2 and 4, with the accompanying receivers in Figures 3 and 5 respectively.

Figure 2 is a functional diagram of a transmitter illustrating the filter method of achieving SSSC. It was indicated earlier that the major problem of this method was the sharp cut-off characteristics required of the filter. This is, of course, true only if a single modulator and filter are used. The transmitter in Figure 2 overcomes the difficulty by using several subcarriers, modulators, and associated bandpass filters. This has the effect of opening a gap in the frequency spectrum between the pass band and the band one most desires to suppress. Hence, the high frequency filters need not have very sharp cut-off characteristics. Slight imperfections in the low frequency filter

result in vestigial sideband operation. An obvious weakness in the transmitter is the need for stabilization of three oscillators instead of one.

The receiver in Figure 3 is an ordinary AM receiver with the beat frequency oscillator serving to re-inject a sub-carrier. With voice modulated input, the receiver must be tuned very carefully since the intelligence is in a band half as wide as usual. Oscillator drift is of more serious consequence. In actual practice, it is found desirable to use the BFO as a fine tuning control. It is to be noted that there is a vestige of lower sideband present in the transmitter output and this may cause cross-channel interference.

The transmitter and receiver in Figures 2 and 3 were adapted from the Western Electric multiplex system, which is also filter type SS operation. Figures 4 and 5 sketch functional diagrams of the system for single channel operation.

Several characteristics of this system are noteworthy:

1. Limiting the lowest modulating frequency to 300 cps separates upper and lower sidebands by a 600 cps guard channel and simplifies filtering out one set of sidebands.
2. Balanced modulators are used for carrier suppression.
3. Crystal filters with very sharp cut-off characteristics are used to suppress one set of sidebands.
4. Subcarriers, multiple modulators and filters are

used to ease the requirements on any one filter.

5. The carrier is not suppressed. On the contrary, it is specifically re-inserted after suppression but at much reduced power level relative to the sidebands. This simplifies locking the receiver on the proper frequency.

6. The receiver amplifies the carrier frequency and uses it as a heterodyning frequency with the input signal to obtain the audio sidebands.

This system is not considered suitable for general use because of the lack of flexibility in frequency. Any frequency change requires retuning a large number of circuits. Further, it is quite difficult to design and build the adjustable filters involved with the desired selectivity.

Another means of obtaining SS is called the phase shift method. In ordinary AM, let

(1) $\begin{cases} \omega_c = \text{angular carrier frequency}, \\ \omega_m = \text{angular modulating frequency}, \\ m = \text{modulation index}, \\ E = \text{unmodulated carrier amplitude}. \end{cases}$

Then, the output signal for a single modulating tone is

(2) $e = E(1+m \sin \omega_m t) \sin \omega_c t$

$= E \left[\sin \omega_c t + \frac{1}{2}m \cos(\omega_c - \omega_m)t - \frac{1}{2}m \cos(\omega_c + \omega_m)t\right]$.

To achieve SS, one constructs two voltages,

(3) $e_1 = e$ and

$$(4)\quad e_2 = E\left[1+m\sin(\omega_m t+90^\circ)\right]\sin(\omega_c t+90^\circ)$$
$$= E\left[\sin(\omega_c t+90^\circ) - \frac{m}{2}\cos(\omega_c t+90^\circ-\omega_m t-90^\circ) - \frac{m}{2}\cos(\omega_c t+90^\circ+\omega_m t+90^\circ)\right]$$
$$= E\left[\cos\omega_c t - \frac{m}{2}\cos(\omega_c-\omega_m)t + \frac{m}{2}\cos(\omega_c+\omega_m)t\right].$$

Then, from (2) and (4)

$$(5)\quad e_2 \pm e_1 = E\left[\cos\ \omega_c t \pm \sin\omega_c t + m\cos(\omega_c \mp \omega_m)t\right].$$

This contains carrier and whichever set of sidebands one desires. To obtain SSSC, one suppresses the carrier in (2) and (4) by means of balanced modulators, for example, and has

$$(6)\quad \bar{e}_1 = \frac{m}{2}E\left[\cos(\omega_c-\omega_m)t - \cos(\omega_c+\omega_m)t\right] ,$$
$$(7)\quad \bar{e}_2 = \frac{m}{2}E\left[\cos(\omega_c-\omega_m)t + \cos(\omega_c+\omega_m)t\right] ,$$
$$(8)\quad \bar{e}_2 \pm \bar{e}_1 = mE\cos(\omega_c \mp \omega_m)t .$$

Such a single sideband system was devised in 1925 (Hartley 12). The important element of the phase shift method of SS is the device which shifts the phase of every modulating frequency voltage 90°. Hartley employs multisection filters of complex design. Byrne improved somewhat on Hartley's system but left much to be desired (Byrne 3). Modern lattice network design reduced the complexity of the system (Cheek 8, Dome 10, Honnell 13). There are two such networks currently in wide use. One has small amplitude errors and large phase angle errors (Dome 10), the other has large amplitude errors and small phase angle errors (Cheek 8, Honnell 13).

The phase shift method leads to a relatively cheap SS transmitter and presently is enjoying a great vogue (Cheek 7 and 8, Dawley 9, Lenehan 14, Nichols 16, Norgaard 17, 18 and 19). Such a system is sketched in Figure 6. The chief difficulty is in the requirement that the phase shift network used in constructing e_2 in (4) from e_1 in (2) must shift the modulating signal phase 90° for every ω_m in the modulation spectrum. In actual practice, this requirement has as yet been impossible to satisfy. However, several phase shifting networks have been designed which yield a "constant" 90° shift to a remarkably good approximation over a frequency band wide enough for intelligibility. Practice has indicated that if the modulating frequencies phase shifter yields an approximate 90° phase shift to within 5° the resulting distortion is not too serious.

Some advantage may be gained by the use of two phase shift networks, one imposing a phase shift $\phi_\alpha = 180^\circ - \alpha$, the other a phase shift $\phi_\beta = 180^\circ + \beta$, neither α nor β being constant with frequency but such that $\phi_\beta - \phi_\alpha = \alpha + \beta$ is approximately 90° over the modulating frequency range. The most important requirement is that the α and β networks share the work and have virtually compensating errors.

This system of operation is illustrated in Figure 7. Of course, (6), (7) and (8) must be modified as follows:

$$
\begin{cases}
e_\alpha = m \sin(\omega_m t - \alpha),\ e_\beta = m \sin(\omega_m t + \beta),\ \alpha + \beta = 90^\circ; \\
\overline{\overline{e}}_1 = mE \sin(\omega_m t - \alpha) \sin \omega_c t = \tfrac{1}{2} mE \left[\cos(\omega_c t - \omega_m t + \alpha) - \cos(\omega_c t + \omega_m t - \alpha)\right], \\
\overline{\overline{e}}_2 = mE \sin(\omega_m t + \beta) \sin(\omega_c t + 90^\circ) = \tfrac{1}{2} mE \left[\cos(\omega_c t - \omega_m t - \beta + 90^\circ) - \cos(\omega_c t + \omega_m t + \beta + 90^\circ)\right] \\
\quad = \tfrac{1}{2} mE \left[\cos(\omega_c t - \omega_m t - \alpha) - \cos(\omega_c t + \omega_m t + 180^\circ - \alpha)\right] \\
\quad = \tfrac{1}{2} mE \left[\cos(\omega_c t - \omega_m t - \alpha) + \cos(\omega_c t + \omega_m t - \alpha)\right], \\
\overline{\overline{e}}_2 \pm \overline{\overline{e}}_1 = mE \cos(\omega_c t \mp \omega_m t \pm \alpha).
\end{cases} \tag{9}
$$

It is readily seen that considerable care must be devoted to the design of the balanced phase shift networks.

It is easy to analyze the distortion effects introduced by imperfect functioning of the modulating frequency phase shifter. For a single modulating tone, let us suppose that we have e_1 as in (2) and that we have in place of (4)

$$
\begin{aligned}
e_2' &= E\left[1 + m \sin(\omega_m t + 90^\circ + \theta)\right] \sin(\omega_c t + 90^\circ) \\
&= E\left[\cos \omega_c t + \tfrac{1}{2} m \cos(\omega_c t - \omega_m t - \theta) + \tfrac{1}{2} m \cos(\omega_c t + \omega_m t + \theta)\right],
\end{aligned}
$$

where θ is small; whence, in suppressed carrier operation,

$$
\begin{aligned}
\overline{e}_2' - \overline{e}_1 &= \tfrac{1}{2} mE \left[\cos(\omega_c t + \omega_m t) + \cos(\omega_c t + \omega_m t + \theta) + \cos(\omega_c t - \omega_m t - \theta) - \cos(\omega_c t - \omega_m t)\right] \\
&= mE \left[\sin(\omega_c t - \omega_m t - \tfrac{1}{2}\theta) \sin \tfrac{1}{2}\theta + \cos(\omega_c t + \omega_m t + \tfrac{1}{2}\theta) \cos \tfrac{1}{2}\theta\right],
\end{aligned}
$$

and similarly

$$
\overline{e}_2' + \overline{e}_1 = mE \left[\cos(\omega_c t - \omega_m t - \tfrac{1}{2}\theta) \cos \tfrac{1}{2}\theta + \cos(\omega_c t + \omega_m t + \tfrac{1}{2}\theta) \sin \tfrac{1}{2}\theta\right].
$$

It is now readily seen that the ratio of unwanted (V_u) to wanted (V_w) sideband voltage amplitude is simply

$$
V_u / V_w = \left| \tan \tfrac{1}{2} \theta \right|. \tag{10}
$$

If the carrier 90° phase shifter has an angular error θ'

and the modulating frequency 90° phase shifter is perfect, it is established in a similar way that

$$(11) \qquad V_u / V_w = \left| \tan \tfrac{1}{2} \theta' \right| .$$

If both errors are present simultaneously,

$$(12) \qquad V_u / V_w = \left| \frac{\sin \frac{1}{2}(\theta - \theta')}{\cos \frac{1}{2}(\theta + \theta')} \right| .$$

In Figure 8 is represented the maximum tolerable phase shifter error associated with a given rejection level of unwanted sideband.

It is also interesting to determine the vestigial sideband effect caused by unbalance in the gain of the two modulating frequency channels. For a single modulating tone, let e_1 be as in (2) and in place of (4),

$$e_2'' = E\left[1 + m' \sin(\omega_m t + 90°)\right] \sin(\omega_c t + 90°), \qquad m' = m(1+\eta).$$

One can readily verify that

$$\overline{e_2''} \pm \overline{e_1} = mE \cos(\omega_c t \pm \omega_m t) + \tfrac{1}{2}\eta m E\left[\cos(\omega_c + \omega_m)t + \cos(\omega_c - \omega_m)t\right],$$

and

$$(13) \qquad \frac{V_u}{V_w} = \left| \frac{\eta}{2 + \eta} \right| .$$

Unbalances in amplitude of the two carrier frequency channels have no effect provided the unbalance does not cause over-modulation of the lower amplitude carrier. In Figure 8 is indicated the maximum tolerable amplitude unbalance (in %) in the two modulating frequency channels

associated with a given rejection level for unwanted sideband.

There is another type of amplitude distortion caused by variation of gain of the modulating frequency channels with frequency and this must be considered in evaluating various proposed 90° phase shifters for the modulating frequencies.

II. THE DOME WIDEBAND PHASE SHIFT NETWORKS

1. Basic R-C Lattice

The most fundamental of three networks proposed (Dome 10) for producing the desired phase shift is shown in Figure 9 and the equivalent circuit of a single stage is shown in Figure 10. We seek an expression for gain and phase shift in the stage. Note that for a single stage

$$(14)\quad \begin{cases} V_{GK}=V_{vK}+V_{Gv}=(I_1+I_2)R_K=e_g & \text{and} \\ e_{out}=V_{vA}=I_1R+(I_1+I_2)R_K. \end{cases}$$

The mesh equations are

$$(15)\quad \begin{cases} -\mu V_{GK}=\mu\left[e_g-(I_1+I_2)R_K\right]=I_1(2R_K)+I_2(2R_K-r_p) \\ 0=I_1(2R_K+Z)+I_2(2R_K), \end{cases}$$

where

$$(16)\qquad Z=R-j/\omega C.$$

Further,

$$(17)\quad \begin{cases} e_p=-(I_1+I_2)R_K=I_1Z/2, \\ e_k=(I_1+I_2)R_K=-e_p. \end{cases}$$

It is readily seen that

$$(18)\qquad e_{out}=V_{VK}+V_{KA}=e_k+I_1R=e_k+2e_pR/\bar{Z}=e_p(2R/Z-1)=e_p\bar{Z}/Z.$$

Hence, the expression for complex gain,

$$(19)\qquad K=e_p\bar{Z}/(e_gZ).$$

Now, using (17), we rewrite (15) and divide by r_p and Z to obtain

$$(20)\qquad \begin{cases} (e_g+e_p)/r_p=I_2-2e_p/r_p \\ 0=I_1-2e_p/Z. \end{cases}$$

Adding the two equations in (20) and employing (17), we obtain

$$(21)\qquad \mu e_g=-r_pe_p\left(\frac{\mu+2}{r_p}+\frac{2}{Z}+\frac{1}{R_K}\right).$$

Applying (21) to (19), one obtains

$$(22)\qquad \begin{cases} K=\mu\bar{Z}/Z\left[\mu+2+r_p\left(\frac{1}{R_K}+\frac{2\bar{Z}}{|Z|^2}\right)\right]=|K|\angle\phi\,, \\ |K|=\mu\left[\left(\mu+2+\frac{r_p}{R_K}+\frac{2Rr_p}{|Z|^2}\right)^2+\left(\frac{2r_p}{\omega C|Z|^2}\right)^2\right]^{-1/2}\,, \\ \phi=2\arctan 1/\omega RC-\arctan 2r_p/\omega RC|Z|^2\left[\mu+2+\frac{r_p+2Rr_p}{R_K\ \ |Z|^2}\right]. \end{cases}$$

Reference to Figures 6 and 7 and the accompanying analysis evinces the necessary condition that $|K|$ be independent of frequency. Therefore, we impose the condition

$$(23)\qquad |Z|/2>>\min\,(R_K,\ 1/g_m)$$

(which is not explicit in Dome's article, loc. cit., but should be), so that (22) reduces to

$$(24)\quad K=\mu(\mu+2+r_p/R_K)^{-1}Z^{-1}\bar{Z},\ |K|=\mu(\mu+2+r_p/R_K)^{-1};\ \phi=2\arctan 1/\omega RC.$$

In the cascaded stages of Figure 9, we use identical tubes for simplicity. Then, for this cascade,

$$(25)\quad \begin{cases} |Z_n|/2=|R_n-jX_n|/2 >> \min(R_{Kn},\ 1/g_m) \quad (n=1,2), \\ |K|=|K_1|\cdot|K_2|=\mu^2(\mu+2+r_p/R_{K1})^{-1}(\mu+2+r_p/R_{K2})^{-1}, \\ \phi=\phi_1+\phi_2=2(\arctan 1/\omega R_1C_1 - \arctan 1/\omega R_2C_2). \end{cases}$$

Now let

$$(26)\quad \begin{cases} \omega_{01}=1/R_1C_1\ ,\ \omega_{02}=1/R_2C_2, \\ \omega_{02}=a\omega_{01},\quad s=(a+1)/\sqrt{a}\ (\geqq 2). \end{cases}$$

Dome assumes further that $R_1=R_2$, so that $C_1=aC_2$, but this is not necessary except as a simplification. Since (26) implies that

$$(27)\quad \omega_{01}=\omega_0/\sqrt{a}\quad \text{and}\quad \omega_{02}=\omega_0\sqrt{a}\ ,$$

we have

$$(28)\quad \begin{aligned} \phi&=2(\arctan \omega_{01}/\omega\ +\arctan\ \omega_{02}/\omega\ )=2\arctan\frac{\omega(\omega_{01}+\omega_{02})}{\omega^2-\omega_0^2} \\ &=2\arctan\frac{s\omega\omega_0}{\omega^2-\omega_0^2}=\arctan\frac{2s\omega\omega_0(\omega^2-\omega_0^2)}{(\omega^2-\omega_0^2)^2-(s\omega\omega_0)^2}\ . \end{aligned}$$

2. The L-C Lattice

Another phase shifting network (Dome 10) is illustrated

in Figure 11. Again, it is not explicit in Dome's article that the shunting impedances across the tube are so large relative to r_p and R_K that we have virtually

$$(29) \quad e_k = \frac{\mu}{(\mu+2)R_K + r_p} e_g = -e_p \quad .$$

We thus have the equivalent network shown in Figure 12, with

$$(30) \quad e_{out} = V_{VK} + V_{KA} = e_k + V_{KA} .$$

Now, the circuit in Figure 12 is equivalent to that in Figure 13. It is not difficult to deduce that (28) holds again, where the network parameters are so proportioned that

$$(29) \quad 1/L_1C_1 = 1/L_2C_2 = \omega_0^2 \ , \ L_1/L_2 = \omega_0 R_1 C_2 = s$$

which implies that $R_1^2 = \sqrt{L_1L_2/C_1C_2} = L_2/C_1 = L_1/C_2$. (This corrects an error due to Dome (Dome 10)).

3. The R-C Lattice.

Still another phase shifting network (Dome 10) is given in Figure 14. Again, it is not explicit in Dome's article (Dome 10) that the shunting impedances across the tube are so large relative to r_p and R_K that (29) and (30) hold. The circuit in Figure 14 is equivalent to that in Figure 15 and therefore to that in Figure 16. Now, let

$$(30)\quad \begin{cases} \omega_0 = 1/R_1C_1 = 1/R_2C_2 = 1/R_3C_3, \\ C_2 = aC_1,\ C_3 = 4a^2C_1/(1-4a) \text{ (hence, } R_2 = R_1/a,\ R_3 = (1-4a)R_1/4a^2), \\ s = (1-2a)/a,\ a = 1/(s+2) \quad (0 < a < 1/4 \text{ so that } s > 2). \end{cases}$$

Then, once more, (28) is readily dirivable.

4. The Dome Design Procedure.

Before discussing the method used by Dome in obtaining the values of s and ω_0 appearing in (28), we make some general remarks. The remarks made here and in the next section apply equally well if one requires the design for a constant phase shift network of Dome type providing any prescribed phase shift. A 90° phase shift is used here as being of primary interest.

For the α and β networks of Figure 7, we shall take two networks of Dome type. We shall introduce the additional subscript α and β respectively to the notation used above. Since the networks must be balanced as to gain, we must have for the gain amplitudes $|K_\alpha| = |K_\beta|$.

For the two networks, we have respectively

$$(31)\quad \begin{cases} \phi_\alpha = 2 \arctan \dfrac{s_\alpha \omega \omega_{0\alpha}}{\omega^2 - \omega_{0\alpha}^2} = 180^\circ - \alpha, \\ \phi_\beta = 2 \arctan \dfrac{s_\beta \omega \omega_{0\beta}}{\omega^2 - \omega_{0\beta}^2} = 180^\circ + \beta. \end{cases}$$

The net phase shift between the two channels is thus

(32) $\Delta\phi = \phi_\beta - \phi_\alpha = \beta + \alpha$.

We desire that this be 90° for all the modulating frequencies. Certainly, (34) is not independent of frequency and can be made 90° for at most a few isolated values of frequency.

Given the modulating frequency range, $\omega_{lower} \leqq \omega \leqq \omega_{upper}$, the best possible design calls for the following procedure. Consider the function:

(33) $$A = \phi_\beta - \phi_\alpha - 90^\circ = 2\left(\arctan\frac{s_\beta \omega \omega_{o\beta}}{\omega^2 - \omega_{o\beta}^2} - \arctan\frac{s_\alpha \omega \omega_{o\alpha}}{\omega^2 - \omega_{o\alpha}^2} - 45^\circ\right)$$

over the interval $\omega_\ell \leqq \omega \leqq \omega_u$ $(\omega_1 = \omega_{lower},\ \omega_u = \omega_{upper})$. Now A vs ω may be graphed as a four parameter ($s_{o\alpha}$, $s_{o\beta}$, $\omega_{o\alpha}$, $\omega_{o\beta}$) family of curves. For each such curve, there is a maximum deviation of A from zero over the interval (ω_ℓ, ω_u). We seek the particular curve which has the minimum such maximum deviation. This curve is associated with a particular set of parameters. This set gives the <u>best possible</u> design constants.

It may be remarked that if a choice of parameters is to minimize maximum $|A|$, then there should be some value $\omega = \Omega$, such that $\omega_\ell < \Omega < \omega_u$, for which $A = 0$. In fact, since A is a "well behaved" function of ω, one might well suspect that maximum $|A|$ will be minimum if $A = 0$ as often as possible in the interval (ω_1, ω_u).

This is <u>not</u> the line of attack used by Dome (loc. cit.).

11331

Instead, he observes empirically that if

(34) $3 < s < 5$,

then, in (28), ϕ is a fairly linear function of $\log \omega$ over a usably wide frequency band. Further, in the α and β networks, one has approximately

$$(35)\quad \begin{cases} \phi_\alpha = b + \log \omega \\ \phi_\beta = b + \log c\omega \\ \phi_\beta - \phi_\alpha = \log c \end{cases}$$

where b and c are constants. Again, empirical considerations lead to the choice

(36) $s_{0\alpha} = s_{0\beta} = 4$

as giving a "most linear" type of ϕ vs $\log \omega$ curve.

The plot of $\phi_\beta - \phi_\alpha$ vs $\log \omega$ varies, one trusts, about 90°. Dome seeks to make $\phi_\beta - \phi_\alpha = 90°$ in the middle of the frequency interval; i.e., he takes Ω such that $\log \Omega = \frac{1}{2}(\log \omega_u + \log \omega_l)$; i.e., Ω is the geometric mean frequency over the band:

(37) $\Omega = \sqrt{\omega_u \omega_l}$.

For the audio band, this is often taken to be 700 cps.

Dome further specifies that at this mean frequency, the networks share the burden of phase shift, i.e. $\beta = \alpha$ for $\omega = \Omega$. Since $\beta + \alpha = 90°$ for $\omega = \Omega$, one has $\beta = \alpha = 45°$ for $\omega = \Omega$. Hence $\phi_\beta = 225°$ and $\phi_\alpha = 135°$ for $\omega = \Omega$.

Thus, $\frac{1}{2}\phi_\beta = 112.5^\circ$ and $\frac{1}{2}\phi_\alpha = 67.5^\circ$ for $\omega = -\Omega$ and, using (36) in (31), one obtains

$$(38) \qquad \frac{4\Omega\omega_{0\alpha}}{\Omega^2 - \omega_{0\alpha}^2} = 1+\sqrt{2} = -\frac{4\Omega\omega_{0\beta}}{\Omega^2 - \omega_{0\beta}^2} \quad ;$$

whence

$$\begin{cases} \Omega^2 - 4(\sqrt{2}-1)\Omega\omega_{0\alpha} - \omega_{0\alpha}^2 = 0, \\ \Omega^2 + 4(\sqrt{2}-1)\Omega\omega_{0\beta} - \omega_{0\beta}^2 = 0, \end{cases}$$

and

$$\begin{cases} \Omega = \left[2(\sqrt{2}-1) + \sqrt{13-8\sqrt{2}}\right]\omega_{0\alpha} = 2.12699\,\omega_{0\alpha} = d\,\omega_{0\alpha}, \\ \Omega = \omega_{0\beta}/d. \end{cases}$$

Such a choice of parameters as given in (36) and (39) yields, according to Dome, α and β phase shift networks for which maximum $|A|$ is 4° over a band for which upper to lower frequency ratio is almost 28 to 1, for example 130 to 3600 cps. Less deviation or greater bandwidth can be obtained by using several such networks in cascade. Actual computation yields a 4.9° maximum $|A|$ over the band, rather than 4° (see Figure 22).

III. FIRST REFINEMENT OF DOME DESIGN

At first, we shall concern ourselves with a very small extension of the Dome procedure. We shall assume,

as does Dome, that

(40) $s_{0\alpha} = s_{0\beta} = s, \beta = \alpha = 45^\circ$ for $\omega = \Omega = \sqrt{\omega_u \omega_l}$.

Hence,

(41) $$\frac{s\Omega\omega_{0\alpha}}{\Omega^2 - \omega_{0\alpha}^2} = 1+\sqrt{2} = -\frac{s\Omega\omega_{0\beta}}{\Omega^2 - \omega_{0\beta}^2} \quad .$$

In (41), let $\omega_{0\alpha} = g\Omega$, $\omega_{0\beta} = h\Omega$, then

$$g/(1-g^2) + h/(1-h^2) = 0 = (g+h)(1-gh)/(1-g^2)(1-h^2) \quad .$$

Hence, $gh = 1$ and

(42) $$sh/(h^2-1) = 1 + \sqrt{2}, \quad \Omega = \sqrt{\omega_{0\alpha}\omega_{0\beta}} \quad .$$

Thus, in (33), with $x = \omega/\Omega$ and $h > 1$,

$$A = 2\left(\arctan\frac{xhs}{x^2-h^2} - \arctan\frac{xs/h}{x^2-h^{-2}} - 45^\circ\right)$$

$$= 2\left(\arctan\frac{s(h-1/h)x(x^2-1)}{x^4+x^2(s^2-h^2-h^{-2})+1} - 45^\circ\right) \quad ;$$

whence

(43) $$\tfrac{1}{2}A = \arctan B - 45^\circ, \quad B > 0.$$

Applying (42) to (43), we obtain

(44) $$B = \frac{s^2(\sqrt{2}-1)x(x^2+1)}{(x^2-1)^2+2x^2s^2(\sqrt{2}-1)} = \frac{tx(x^2+1)}{x^4+x^2(2t-2)+1}, \quad t=s^2(\sqrt{2}-1)$$

The problem then is one of choosing t in (44) in such a way that for a given maximum $|A|$ the bandwidth is maximum, or for a given bandwidth the maximum $|A|$ is minimum. Each of these is solved in a similar manner. Note that

$$\frac{dB}{dx} = t(1-x^2)\left[x^4+x^2(6-2t)+1\right] \Big/ \left[x^4+x^2(2t-2)+1\right]^2 \quad .$$

and B has an extremum at $y_2 = 1$. This is the only extremum and a maximum if $t \leq 4$. If $t > 4$, then $y_2 = 1$ is a minimum and there are two maxima at

$$(45) \quad y_{1,3} = \sqrt{(t-4)/2} \mp \sqrt{(t-8)/2} \quad .$$

In Figure 17 are sketched typical members of the one parameter (t) family of B vs x curves. It is geometrically evident that the useful curves are those for which $t \geq 4$. There is some simplification in noting that $B(x) = B(1/x)$, so that we need only consider $x > 1$.

It must be remarked that in replacing consideration of deviations of A from zero by consideration of deviations of B from unity, we cannot consider values of $B < 1$ in the same light as values of $B > 1$. Note that if $B_1 = 1+m$ and $B_2 = 1-n$ $(m,n > 0)$, then

$$|A_1|/2 = \arctan B_1 - 45^\circ = 45^\circ - \arctan B_2 = |A_2|/2 \quad \text{if } B_1 = 1/B_2 .$$

Further, if $t > 4$,

$$(46) \quad B_{max}\Big|_{t>4} = \frac{ty_{1,3}^2\sqrt{2t-4}}{2y_{1,3}^2(2t-4)} = t/2\sqrt{2t-4} \quad .$$

At the same time,

$$B\Big|_{\substack{t=4\\x=y_{1,3}}} = \frac{4x(x^2+1)}{x^4+6x^2+1}\Big|_{y_{1,3}} = \frac{4y_{1,3}^2\sqrt{2t-4}}{y_{1,3}^2(2t-4)+4y_{1,3}^2} = 2\sqrt{2t-4}/t = 1/B_{max}\Big|_{t>4}$$

and it becomes geometrically evident that one should take $t > 4$, i.e. $s^2 > 4(\sqrt{2}+1)$.

In fact, given a bandwidth ratio $\omega_u/\omega_l = p^2$, one should take $t > 4$ so that $B(p) = 1/B_{max} = 1/B(y_3)$, i.e.

$$(47)\quad \begin{cases} 2\sqrt{2t-4}/t = tp(p^2+1)/[(p^2+1)^2+p^2(2t-4)] & \text{or} \\ q/u + u/q = (u+u^{-1})^2/2, \quad u=\sqrt{2t-4}/2 > 1, \quad q=(p+p^{-1})/2 > 1. \end{cases}$$

This is geometrically obvious from Figure 17.

Similarly, given a maximum permissible $|A|$, we immediately have a maximum permissible B_{max}. We then seek the largest bandwidth ratio p^2 such that neither B nor 1/B exceeds the maximum permissible B_{max} over the interval $1/p \leqq x \leqq p$. It is geometrically obvious from Figure 17 that this is achieved by taking $B(p) = 1/B_{max}$ again. Thus, (47) serves as a defining equation for p in terms of t, and hence of B_{max}.

The problem of maximum bandwidth for a given maximum permissible deviation and the problem of minimum maximum deviation for a given bandwidth are essentially the same. In fact, one may begin by assigning values to s, then computing t by (44), B_{max} by (46), maximum $|A|$ by (43), bandwidth factor p from (47).

This is the procedure followed in obtaining Figure 18, which indicates the maximum bandwidth obtainable for a given permissible deviation and the minimum maximum deviation obtainable for a given bandwidth. Also, it indicates the choice of design parameter s pertaining to each condition.

IV. SECOND REFINEMENT OF DOME DESIGN

As was seen in (33) we are concerned with the function

$$A = 2(\arctan B - 45^{\circ}),$$

where

$$(48) \quad B(\omega/\Omega) = \frac{\omega\omega_{o\beta}S_\beta(\omega^2-\omega_{o\alpha}^2) - \omega\omega_{o\alpha}S_\alpha(\omega^2-\omega_{o\beta}^2)}{(\omega^2-\omega_{o\beta}^2)(\omega^2-\omega_{o\alpha}^2) + \omega^2\omega_{o\alpha}\omega_{o\beta}S_\alpha S_\beta}, \quad \Omega = \sqrt{\omega_u\omega_\ell}.$$

We seek to minimize maximum $|A|$ over the interval (ω_ℓ, ω_u), which is equivalent to minimizing maximum C-1 where

$$(49) \quad C = B \text{ if } B \geq 1, \quad C = 1/B \text{ if } B \leq 1.$$

Having four parameters at our disposal in (48), we can expect that we can make $B = 1$ for four distinct values of ω in the interval (ω_1, ω_u) and that a best choice of parameters will accomplish this in the process of minimizing maximum C-1.

Unfortunately, as was pointed out in the previous section, the two fundamental assumptions of the Dome method are given by (40). There is no compelling reason for making these assumptions. In fact, the design can be

improved by not making them. For, these very assumptions imply that, of the four values of ω for which $B = 1$ (48), two at least are coincident, since $B = 1$ and $dB/d\omega = 0$ for $\omega = \Omega$. Thus, these assumptions preclude minimalization of maximum C-1.

We can continue further the general remarks concerning the choice of parameters $\omega_{o\alpha}, \omega_{o\beta}, s_\alpha, s_\beta$ in (48). Observing that the desired and obtainable form of B(x) vs x $(= \frac{\omega}{\Omega})$ curve is as shown in Figure 19, we see that the design parameters must be chosen so as to give four distinct values x_1, x_2, x_3, x_4 of x in the interval (1/p, p) for which $B = 1$. Also, there are three distinct values y_1, y_2, y_3 of x in this interval for which B is extreme and these are such that

$$(50) \quad B(y_1) = B(y_3) = 1/B(y_2) > 1 \ , \ B(y_2) = B(p) = B(1/p).$$

The computational difficulties involved in this procedure are perhaps excessive.

However, we can preserve much of the simplicity of calculation of the preceding section by assuming that B(x) is a symmetric function of log ω , i.e. $B(\frac{\omega}{\Omega}) = B(\frac{\Omega}{\omega})$. This has the effect of assuring that the network performance does not favor either high or low frequencies. This symmetry, by the way, is a consequence of Dome's assumptions (40), but the latter imply additional undesired restrictions of the function B.

In the following, it is shown that

(a) $B(x) = B(1/x)$ requires that $s_\alpha = s_\beta$ and $\omega_{o\alpha}\omega_{o\beta} = \Omega^2$ for minimalization of maximum $|A|$.

It can be shown in a similar manner that:

(b) $\omega_{o\alpha}\omega_{o\beta} = \Omega^2$ results in $s_\alpha = s_\beta$ and $B(x) = B(1/x)$,

(c) $s_\alpha = s_\beta$ results in $\omega_{o\alpha}\omega_{o\beta} = \Omega^2$ and $B(x) = B(1/x)$,

for minimalization of maximum $|A|$.

Hence, any one of the three assumptions $B(x) = B(1/x)$, $s_\alpha = s_\beta$ or $\omega_{o\alpha}\omega_{o\beta} = \Omega^2$ may be made with identical results. The remaining case in which one has simultaneously $s_\alpha \neq s_\beta$, $\omega_{o\alpha}\omega_{o\beta} \neq \Omega^2$, and $B(x) \neq B(1/x)$ for every x in $(1/p, p)$ has not been investigated fully because of the complexity. However, there is strong evidence that maximum $|A|$ is minimized only if $B(x) = B(1/x)$.

In order to simplify manipulation, we introduce into (48) the substitutions used in the previous section:

$$(51)\quad \Omega = \sqrt{\omega_u \omega_l} \ , \ \omega_{o\alpha} = g\Omega, \ \omega_{o\beta} = h\Omega \ , \ \omega = x\Omega \ , \ 1/p \leqq x \leqq p = \sqrt{\omega_u/\omega_l}$$

Then,

$$(52)\quad B(x) = \frac{x\left[x^2(hs_\beta - gs_\alpha) + gh(hs_\alpha - gs_\beta)\right]}{x^4 + x^2(ghs_\alpha s_\beta - g^2 - h^2) + g^2h^2}$$

The symmetry condition requires that $B(x) = B(1/x)$. Comparing coefficients of like powers of x, one obtains

$$(53)\quad s_\beta (h^2+1)/h = s_\alpha(g^2+1)/g \quad \text{and either } g = h \text{ or } gh = 1 \text{ or}$$
$$s_\alpha = (h^2+1)/h, \ s_\beta = (g^2+1)/g.$$

If $g = h$, then $s_\alpha = s_\beta$ and $B(x) = 0$, which is absurd. Hence,

$g \neq h$. If $s_\alpha = (h^2+1)/h$ and $s_\beta = (g^2+1)/g$, then $B(x) = x(h^2-g^2)/gh(x^2+1)$ and this function is not of the form shown in Figure 19 but has but a single maximum as shown in Figure 20. Therefore,

(54) $gh = 1$.

Hence, in (53),

(55) $s_\alpha = s_\beta = s$,

and thus, in (52),

(56) $$B(x) = \frac{su\,x(x^2+1)}{x^4+x^2(s^2-u^2-2)+1} \qquad (h > 1/h = g,\ u = h-g > 0).$$

We shall need also

(57) $$\frac{dB}{dx} = su(1-x^2)\left[x^4-x^2(s^2-u^2-6)+1\right]/\left[x^4+x^2(s^2-u^2-2)+1\right]^2 .$$

In order for $B(x)$ to have the three distinct extrema of Figure 19, we must have

(58) $s^2-u^2 > 8$.

Then, $y_2 = 1$ is a minimum point and

(59) $$y_{1,3} = \tfrac{1}{2}\sqrt{s^2-u^2-4} \mp \tfrac{1}{2}\sqrt{s^2-u^2-8}$$

are maximum points. Thus, to satisfy (50), we must have

(60) $$\begin{cases} B(y_{1,3}) = su/2\sqrt{s^2-u^2-4} = 1/B(y_2) , \\ B(y_2) = 2su/(s^2-u^2) = sup(p^2+1)/\left[p^4+p^2(s^2-u^2-2)+1\right] . \end{cases}$$

From (60),

$$(61)\qquad \begin{cases} s^2-u^2 = 2(p+1)^2/p = r_1 \ , \\ su = \left[(p+1)/p\right]\sqrt[4]{8p(p^2+1)} = r_2 \ , \end{cases}$$

whence,

$$(62)\qquad \begin{cases} u = \sqrt{(p+1)\left[\sqrt{p^2+1}+\sqrt{2p}-(p+1)\right]/p} \\ s = \sqrt{(p+1)\left[\sqrt{p^2+1}+\sqrt{2p}+(p+1)\right]/p} \\ B(y_2) = \sqrt{2}\,\sqrt[4]{2p(p^2+1)}\,/(p+1) \\ \min\max|A| = 2\left[\arctan\dfrac{p+1}{\sqrt[4]{8p(p^2+1)}} - 45^\circ\right]. \end{cases}$$

Figure 21 shows the relationship between bandwidth factor p and the minimum maximum deviation from constant 90° phase shift over the interval of modulating frequencies. Figure 18 is replotted in Figure 21 to serve as a basis for comparison. The improvement is evident.

Dome (Dome 10; page 114) gives the design constants for an R-C lattice based on (36), (38), (39) above. This network was built and its phase shift characteristics studied. Also, an identical network to cover the same frequency band was built using the improved design procedure. The phase shift characteristics of both networks are plotted for comparison in Figure 22.

It is seen that a 3.6° maximum error is obtained with the improved design, a 4.9° error with Dome's design for

the same operating band. As seen from Figure 21, if a 4.9° maximum error were tolerable, with the improved design one could extend the acceptable operating band from Dome's 130-3600 cps to 108-4550 cps, i.e. from $\frac{\omega_u}{\omega_\ell} = 27.8$ to 42.25.

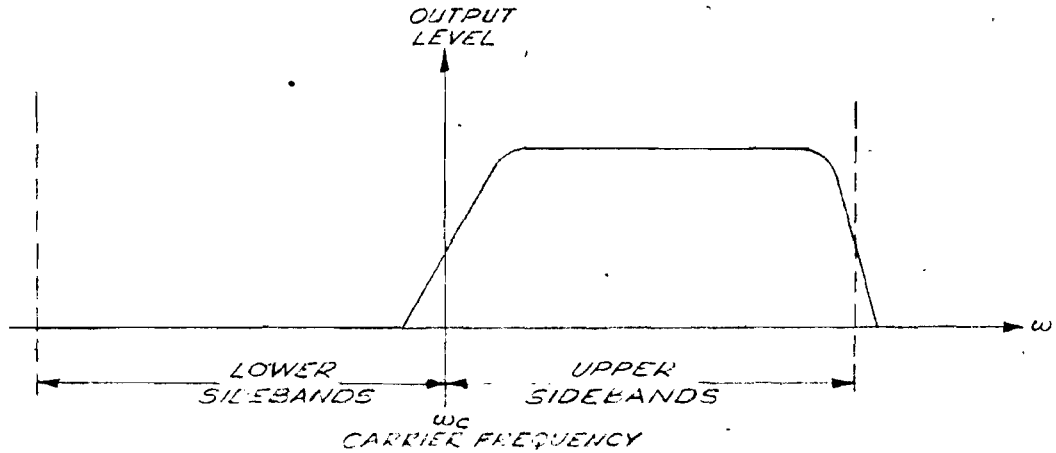

FIGURE 1: OUTPUT LEVEL VS. FREQUENCY OF SIDEBAND AND CARRIER FOR UNIFORM MODULATION LEVEL IN VESTIGIAL SIDEBAND OPERATION

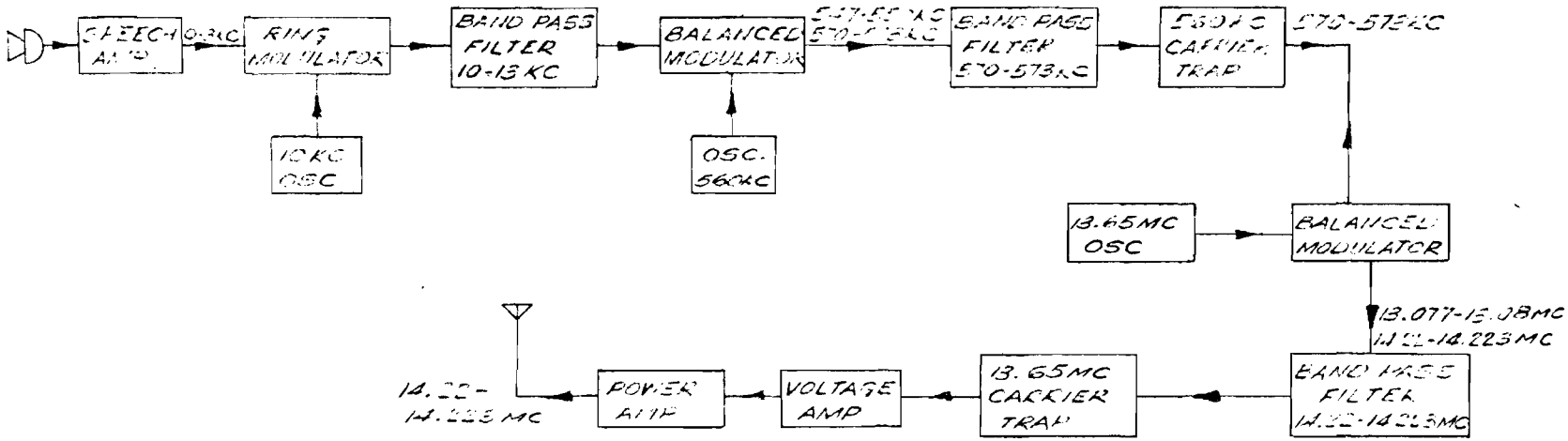

FIGURE 2: FILTER TYPE SS TRANSMITTER

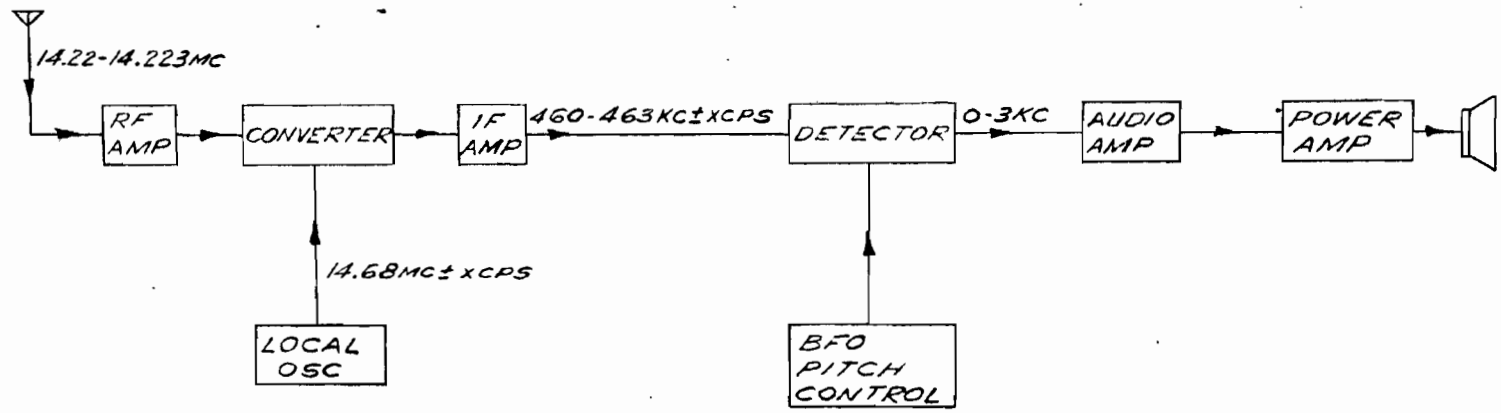

FIGURE 3: SIMPLE SS RECEIVER

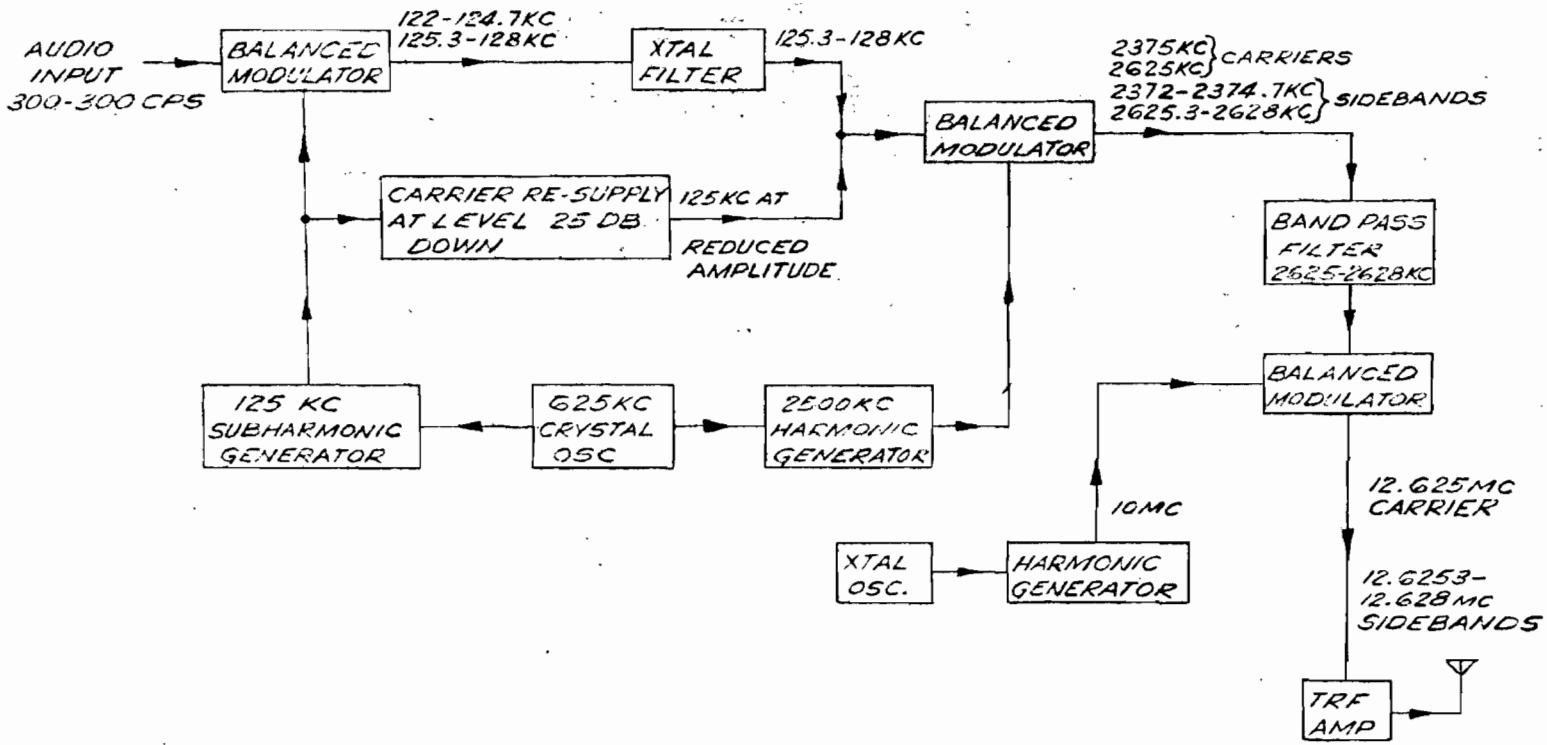

FIGURE 4: WESTERN ELECTRIC 55 TRANSMITTER

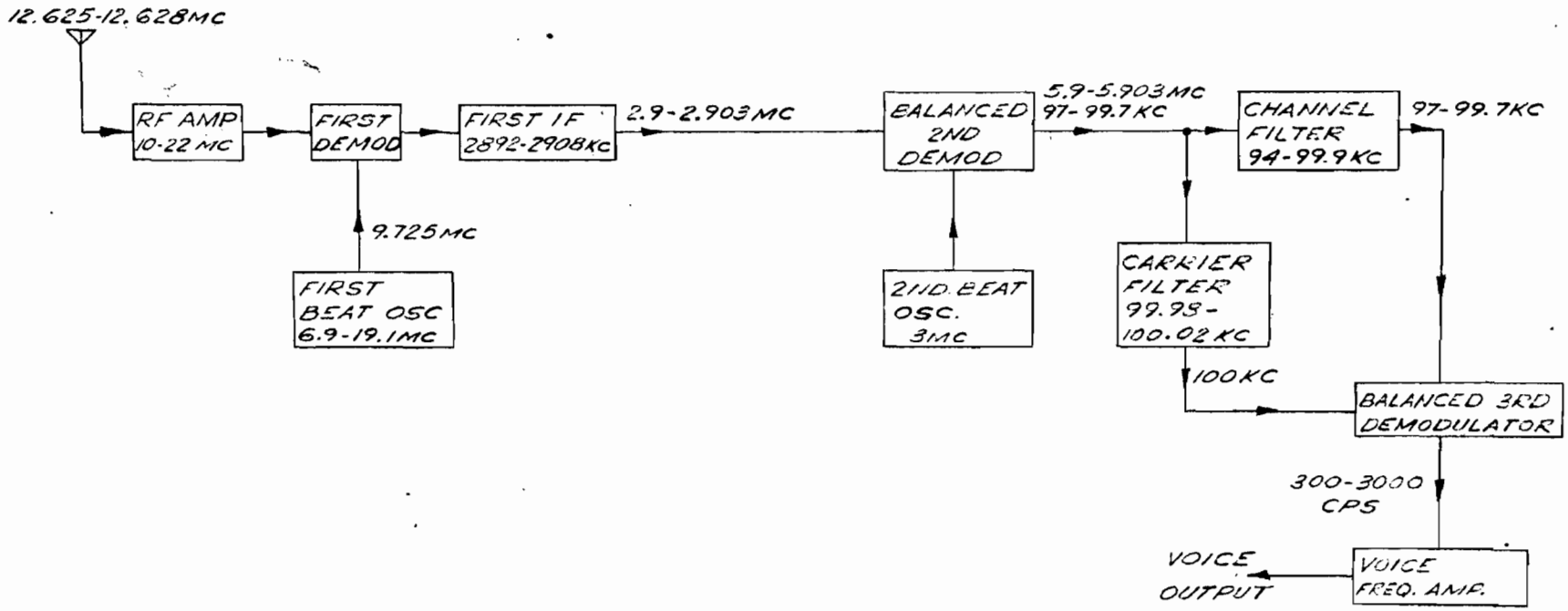

FIGURE 5: WESTERN ELECTRIC CO. 55 RECEIVER

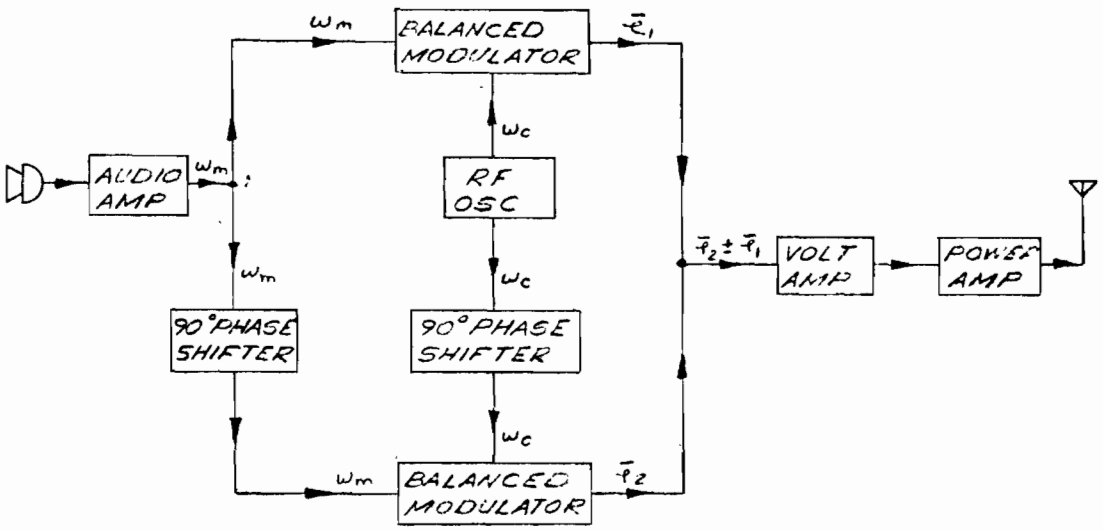

FIGURE 6: PHASE SHIFT SSSC TRANSMITTER

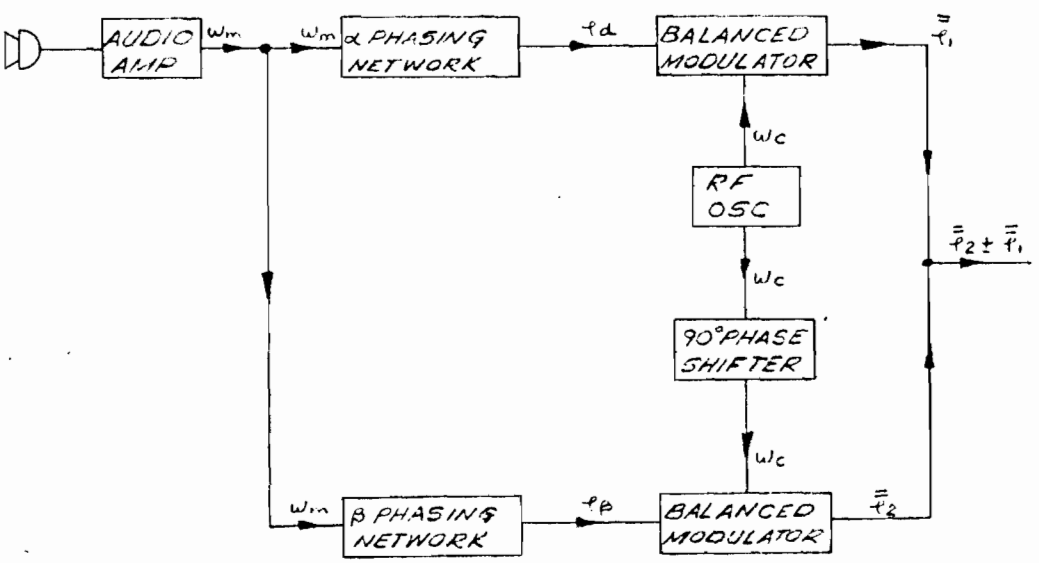

FIGURE 7: BALANCED PHASE SHIFT SSSC TRANSMITTER

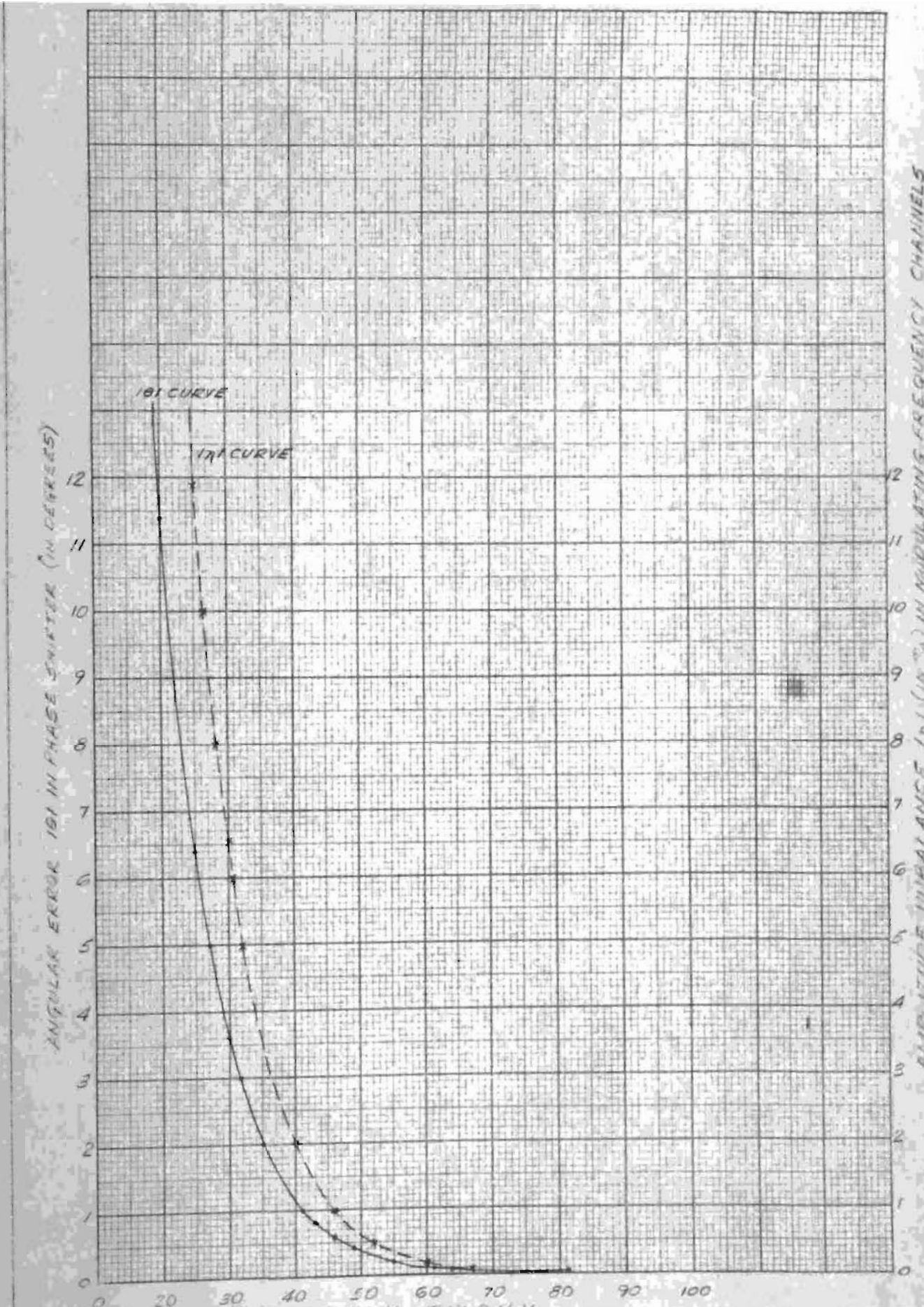

FIGURE 5: VESTIGIAL SIDEBAND EFFECTS IN PHASE & 181 SSEC SYSTEM

SIGNATURE _____ DATE _____ CURVE NO. _____

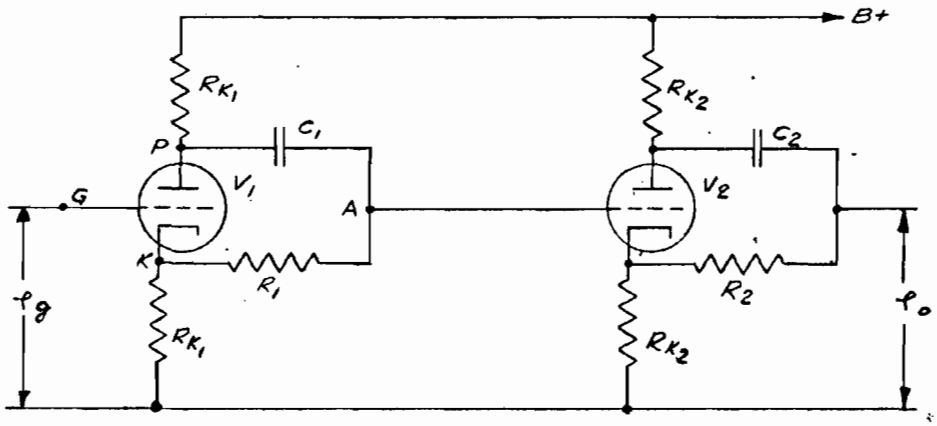

FIGURE 9 BASIC R-C LATTICE

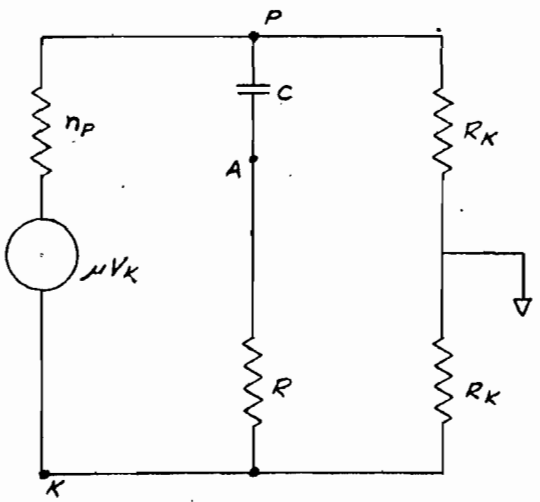

FIGURE 10: EQUIVALENT CIRCUIT OF BASIC R-C LATTICE SINGLE STAGE

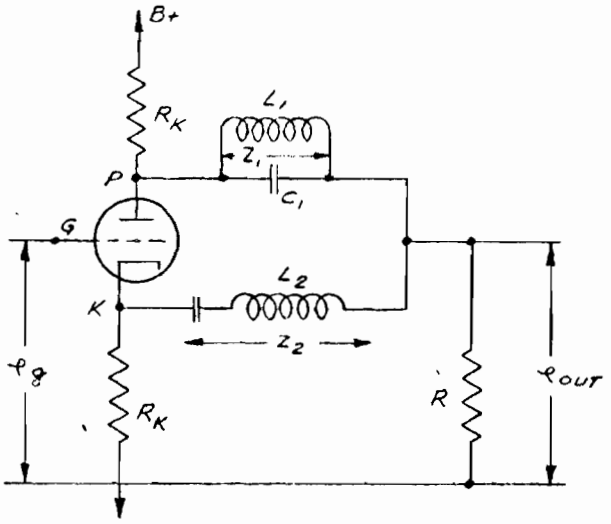

FIGURE 11: L-C LATTICE

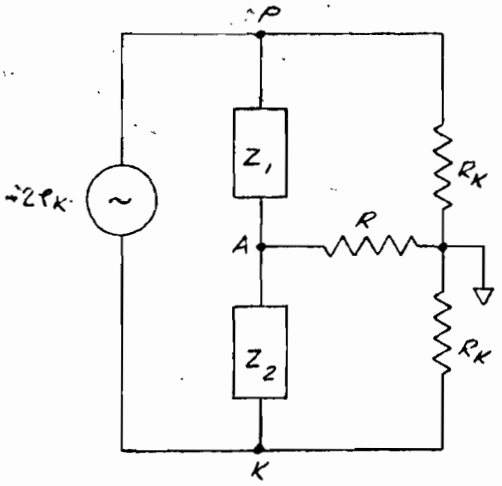

FIGURE 12

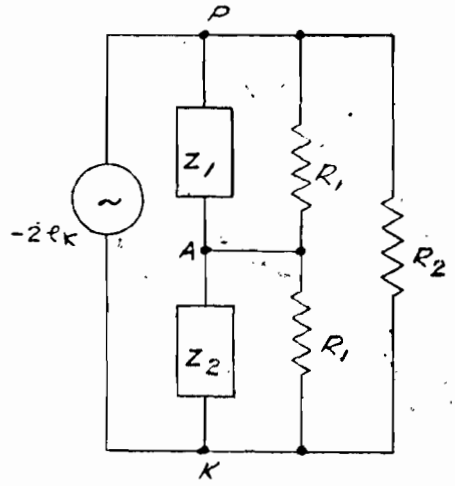

FIGURE 13

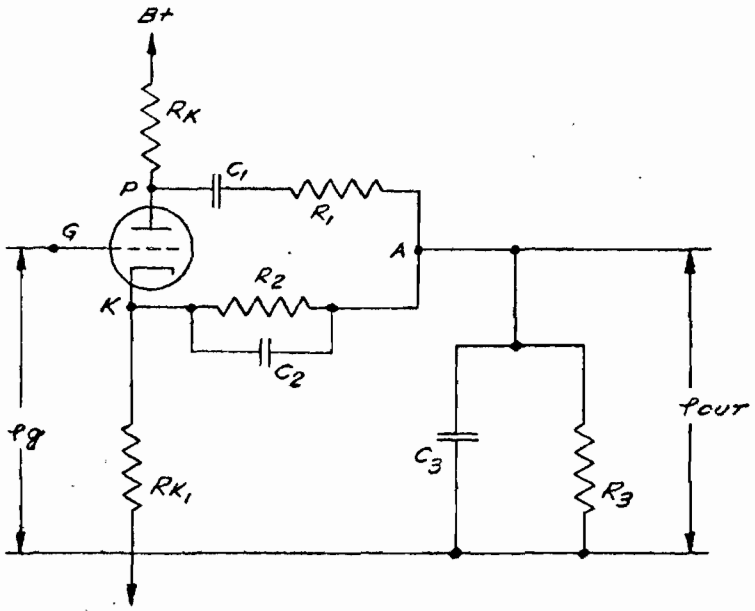

FIGURE 14: R-C LATTICE

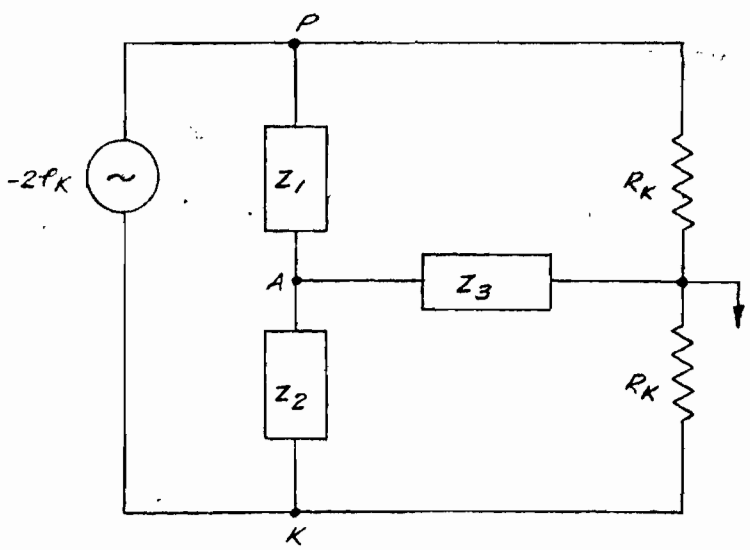

FIGURE 15

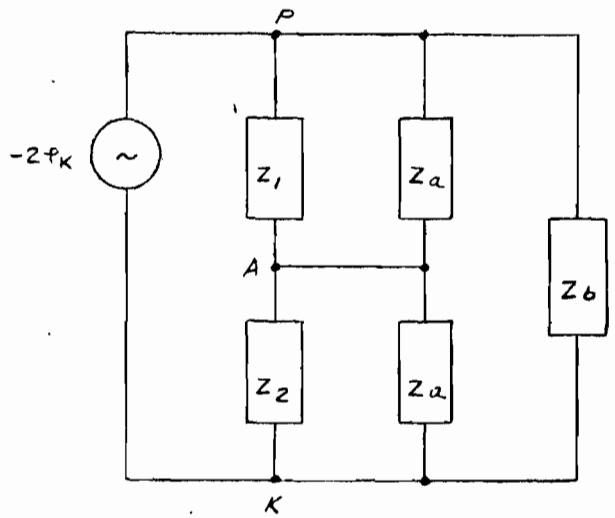

FIGURE 16

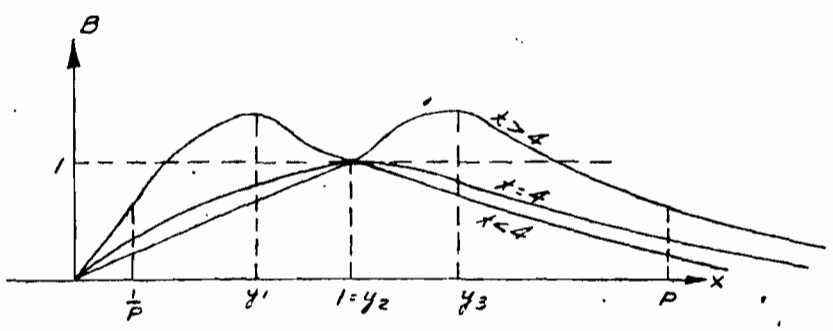

FIGURE 17

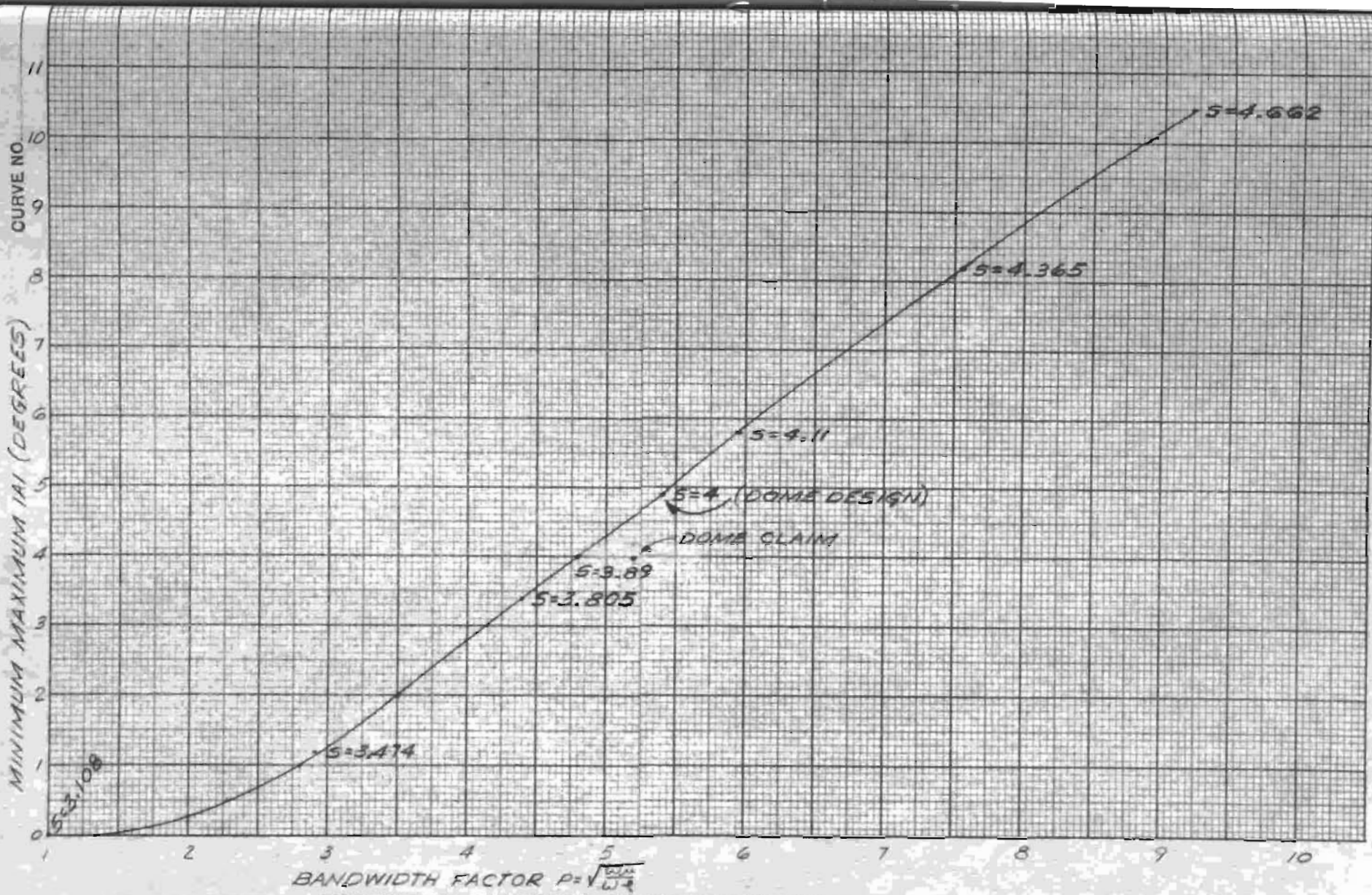

FIGURE 18: EXTENSION OF DOME DESIGN PROCEDURE

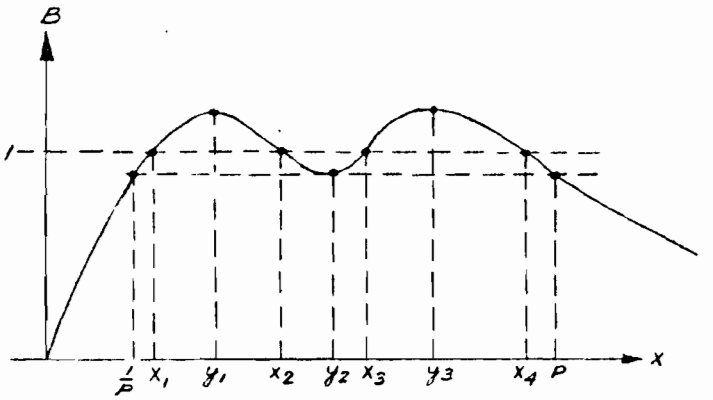

FIGURE 19

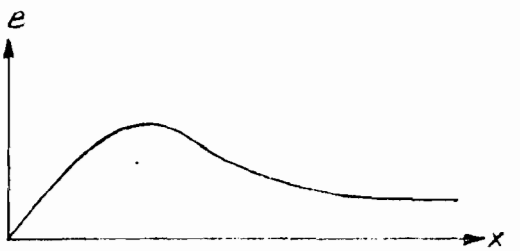

FIGURE 20

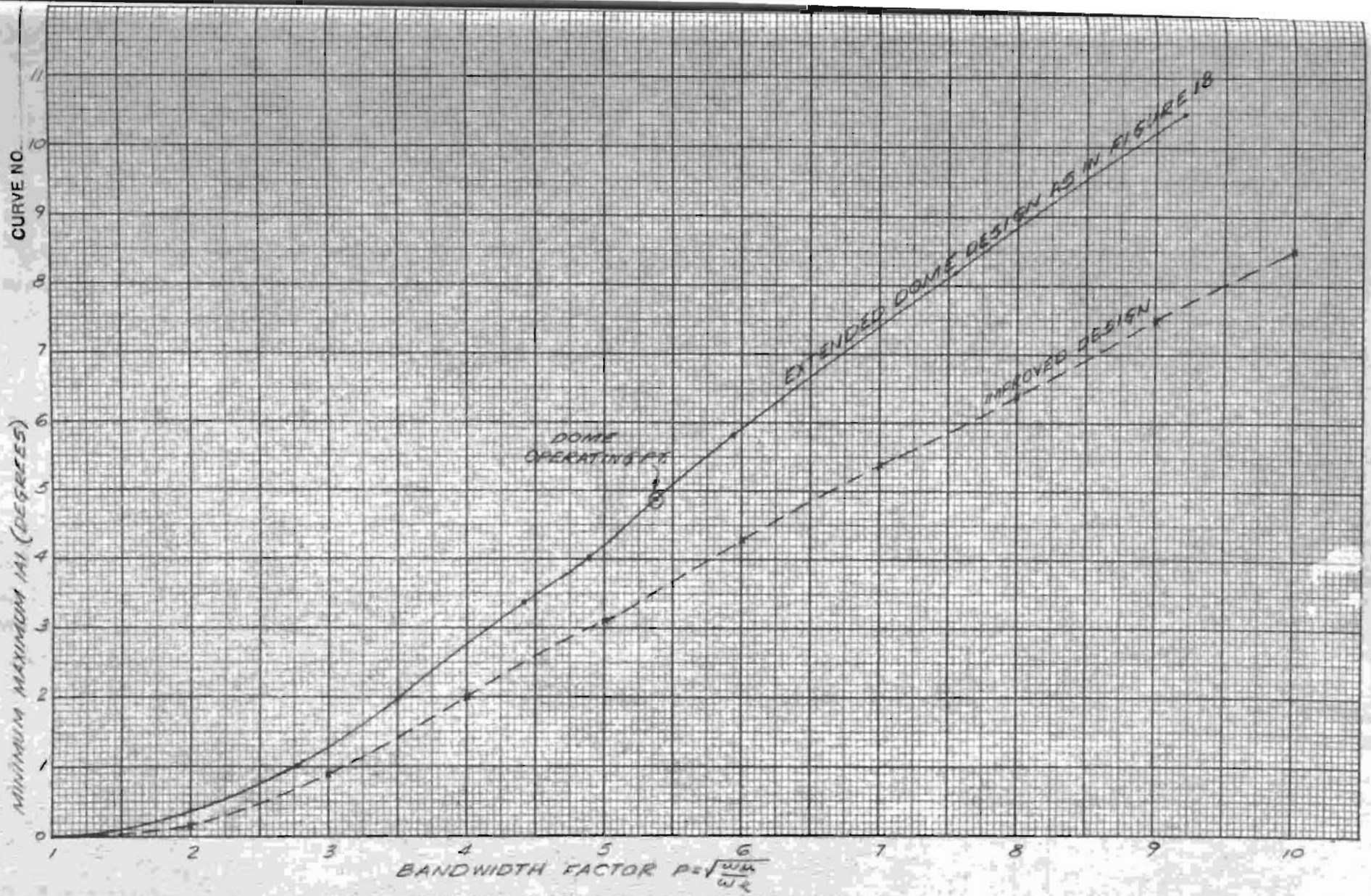

FIGURE 21: FURTHER EXTENSION OF DOME DESIGN

FIGURE 22: COMPARISON OF IDENTICAL PHASE SHIFT NETWORKS WITH DIFFERENT DESIGN PROCEDURE

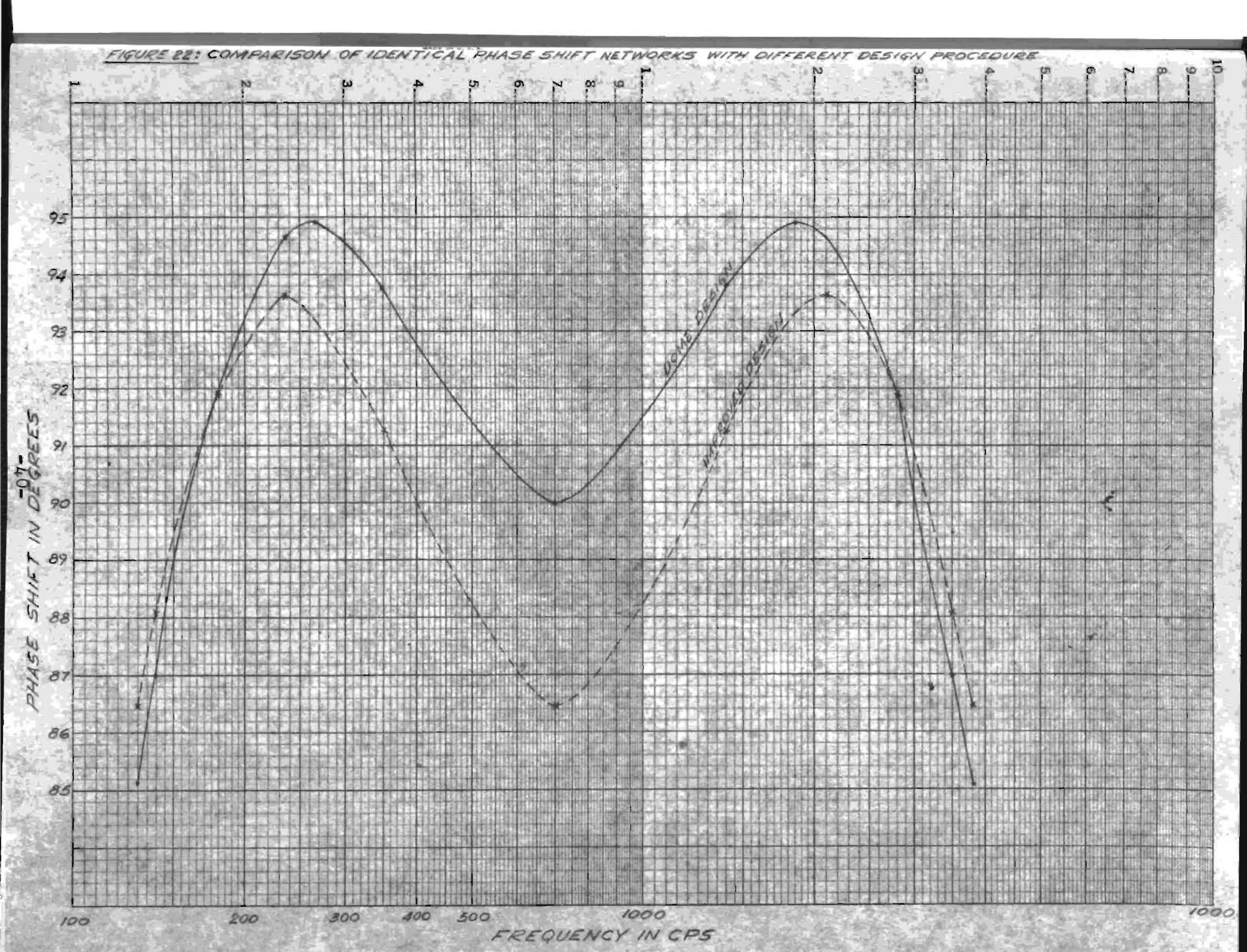

BIBLIOGRAPHY

1. Almquist, M.L., Fisher, H.J., and Mills, R.H. A new single channel carrier telephone system. American Institute of Electrical Engineering, volume 57, 1938, pp. 25-33, pp. 227ff.

2. Blackwell, O.B., and Colpitts, E.H. Carrier current telephony and telegraphy. American Institute of Electrical Engineering, volume 40, 1921, pp. 205-300.

3. Byrne, J.F. Polyphase broadcasting. American Institute of Electrical Engineering, volume 58, 1939, pp. 347-350.

4. Carson, J.R. U.S. Patent 1,449,382.

5. Cheek, R.C. Power line carrier modulation system. Westinghouse Engineer. March 1945.

6. Cheek, R.C. A comparison of the AM, FM and single sideband systems for power line carrier transmission. Westinghouse Technical Data 85-700. Transactions, American Institute of Electrical Engineering, May 1945.

7. Cheek, R.C. A simple single sideband carrier system. Westinghouse Engineer, November 1945.

8. Cheek, R.C. Single sideband for everyone. CQ, November 1948, pp. 17-22, 93-96.

9. Dawley, R.L. An SSSC transmitter adapter. QST, July 1948.

10. Dome, R.B. Wideband phase shift networks. Electronics, December 1946, pp. 112-115.

11. General Electric Ham News. Volume 3, number 6, November-December 1948.

12. Hartley, R.V.L. U.S. Patent 1,666,206.

13. Honnell, M. Single sideband generator. Electronics, November 1945, pp. 166-168.

14. Lenehan, B.E. Electrical Engineering, volume 66, June 1947, pp. 549-552.

15. Moore, R.M. Single sideband transmission. R/9 Sept.-Oct., Dec. 1933, Jan.-Feb. 1934.

16. Nichols, A.H. Single sideband transmitter for amateur operation. QST, January 1948.

17. Norgaard, D.E. What about single sideband? QST, May 1948.

18. Norgaard, D.E. New approach to single sideband. QST, June 1948.

19. Norgaard, D.E. Practical single sideband reception. QST, July 1948.